On the basis of the evidence presented in this report, we propose that appressoria of the rice blast fungus infect plants by using a septin-dependent mechanism summarized in Fig. 4G. In this model, isotropic expansion of the pressurized appressorium is directed into mechanical force at the base of the infection cell. This is dependent on assembly of an extensive toroidal F-actin network at the appressorium pore to provide cortical rigidity at the initially wall-less region of the appressorium. Septins organize the actin network, making direct phosphoinositide linkages to the plasma membrane and facilitating the action of ERM proteins, such as Tea1, which link cortical F-actin to the membrane. The septin ring also acts as a diffusion barrier to ensure localization of proteins, such as the Rvs167 I-BAR protein, and the WASP/WAVE complex involved in membrane curvature at the tip of the emerging penetration peg and F-actin polymerization (Fig. 4G). In this way, the rice blast fungus extends a rigid penetration peg that ruptures the leaf cuticle and invades the host plant tissue.

References and Notes

1. J. C. de Jong, B. J. McCormack, N. Smirnoff, N. J. Talbot, *Nature* **389**, 244 (1997).
2. T. M. Bourett, R. J. Howard, *Can. J. Bot.* **68**, 329 (1990).
3. C. Bechinger *et al.*, *Science* **285**, 1896 (1999).
4. A. Berepiki, A. Lichius, J. Y. Shoji, J. Tilsner, N. D. Read, *Eukaryot. Cell* **9**, 547 (2010).
5. A. S. Gladfelter, L. Kozubowski, T. R. Zyla, D. J. Lew, *J. Cell Sci.* **118**, 1617 (2005).
6. R. Lindsey, M. Momany, *Curr. Opin. Microbiol.* **9**, 559 (2006).
7. L. M. Douglas, F. J. Alvarez, C. McCreary, J. B. Konopka, *Eukaryot. Cell* **4**, 1503 (2005).
8. E. T. Spiliotis, W. J. Nelson, *J. Cell Sci.* **119**, 4 (2006).
9. L. H. Hartwell, *Exp. Cell Res.* **69**, 265 (1971).
10. D. G. Saunders, Y. F. Dagdas, N. J. Talbot, *Plant Cell* **22**, 2417 (2010).
11. G. A. Castillon *et al.*, *Curr. Biol.* **13**, 654 (2003).
12. D. G. Saunders, S. J. Aves, N. J. Talbot, *Plant Cell* **22**, 497 (2010).
13. C. Veneault-Fourrey, M. Barooah, M. Egan, G. Wakley, N. J. Talbot, *Science* **312**, 580 (2006).
14. E. Bi *et al.*, *J. Cell Biol.* **142**, 1301 (1998).
15. A. E. Adams, D. I. Johnson, R. M. Longnecker, B. F. Sloat, J. R. Pringle, *J. Cell Biol.* **111**, 131 (1990).
16. I. Sagot, S. K. Klee, D. Pellman, *Nat. Cell Biol.* **4**, 42 (2002).
17. M. Versele, J. Thorner, *J. Cell Biol.* **164**, 701 (2004).
18. L. Li, K. Xue, K. Bruno, M. Nishimura, J. R. Xu, *Mol. Plant Microbe Interact.* **17**, 547 (2004).
19. J. R. Xu, C. J. Staiger, J. E. Hamer, *Proc. Natl. Acad. Sci. U.S.A.* **95**, 12713 (1998).
20. G. Park, C. Xue, L. Zheng, S. Lam, J. R. Xu, *Mol. Plant Microbe Interact.* **15**, 183 (2002).
21. J. Gilden, M. F. Krummel, *Cytoskeleton* **67**, 477 (2010).
22. B. T. Fievet *et al.*, *J. Cell Biol.* **164**, 653 (2004).
23. A. Casamayor, M. Snyder, *Mol. Cell. Biol.* **23**, 2762 (2003).
24. M. Onishi *et al.*, *Mol. Cell. Biol.* **30**, 2057 (2010).
25. M. Iwase *et al.*, *Mol. Biol. Cell* **17**, 1110 (2006).
26. Y. Barral, V. Mermall, M. S. Mooseker, M. Snyder, *Mol. Cell* **5**, 841 (2000).
27. P. A. Takizawa, J. L. DeRisi, J. E. Wilhelm, R. D. Vale, *Science* **290**, 341 (2000).
28. H. Zhao, A. Pykäläinen, P. Lappalainen, *Curr. Opin. Cell Biol.* **23**, 14 (2011).
29. M. J. Egan, Z. Y. Wang, M. A. Jones, N. Smirnoff, N. J. Talbot, *Proc. Natl. Acad. Sci. U.S.A.* **104**, 11772 (2007).
30. P. K. Mattila *et al.*, *J. Cell Biol.* **176**, 953 (2007).
31. T. Takenawa, S. Suetsugu, *Nat. Rev. Mol. Cell Biol.* **8**, 37 (2007).
32. A. Madania *et al.*, *Mol. Biol. Cell* **10**, 3521 (1999).

The *lac* Repressor Displays Facilitated Diffusion in Living Cells

Petter Hammar, Prune Leroy, Anel Mahmutovic, Erik G. Marklund, Otto G. Berg, Johan Elf*

Transcription factors (TFs) are proteins that regulate the expression of genes by binding sequence-specific sites on the chromosome. It has been proposed that to find these sites fast and accurately, TFs combine one-dimensional (1D) sliding on DNA with 3D diffusion in the cytoplasm. This facilitated diffusion mechanism has been demonstrated in vitro, but it has not been shown experimentally to be exploited in living cells. We have developed a single-molecule assay that allows us to investigate the sliding process in living bacteria. Here we show that the *lac* repressor slides 45 ± 10 base pairs on chromosomal DNA and that sliding can be obstructed by other DNA-bound proteins near the operator. Furthermore, the repressor frequently (>90%) slides over its natural *lacO₁* operator several times before binding. This suggests a trade-off between rapid search on nonspecific sequences and fast binding at the specific sequence.

Transcription factors (TFs) have evolved to rapidly find their specific binding sites among millions of nonspecific sites on chromosomal DNA (*1*). In 1970, Riggs *et al.* showed that in vitro the *lac* repressor (LacI) finds its operator apparently faster than the rate limit for three-dimensional (3D) diffusion (*2*). These experiments were explained by the facilitated diffusion theory (*3*, *4*), which posits that TFs search for their binding sites through a combination of 3D diffusion in the cytoplasm and 1D diffusion (sliding) along the DNA. The sliding effectively extends the target region to the sliding distance, which facilitates the search process. Since then, sliding on DNA has been studied in various in vitro assays (*5–8*), including direct observations in single-molecule experiments (*9*, *10*). However, the physiological relevance of the long sliding distances observed at low salt concentrations in vitro has been questioned (*11*, *12*). This is because the high intracellular concentrations of salt and nucleoid proteins are expected to reduce sliding distances (*13*). Therefore, whether facilitated diffusion is used in living cells, and if so, how far a TF slides on chromosomal DNA, remain unanswered questions.

Single-molecule imaging provides the time resolution necessary to study TF binding kinetics in living cells. Using a yellow fluorescent protein–labeled LacI in *Escherichia coli* cells, we developed an assay for measuring the search time based on the distinction between localized and diffuse fluorescence signals (*14*). On a 4-s time scale, individual operator-bound LacI-Venus molecules appear as diffraction-limited spots over the background of freely diffusing molecules (Fig. 1A). By measuring the average number of fluorescent spots per cell as a function of time after removing the inducer isopropyl-β-D-1-thiogalactopyranoside (IPTG) (fig. S7), the kinetics of TF binding to an individual operator site in the *E. coli* chromosome can be monitored at a time resolution of seconds (Fig. 1B) (*15*). The fusion to Venus prevents LacI from forming tetramers, thus removing the possibility that the protein will loop DNA. The accuracy of the assay depends on limiting the total number of repressors to three to five molecules per cell (*14*, *16*). This can be achieved (fig. S6) by increasing the autorepression through a single artificial lacO_sym operator site partially overlapping the repressor coding region (Fig. 1B, inset).

When we measured the association rate in the strain with a single *lacO_sym* (JE101), we found that it took an average time of 56 ± 2 s (SEM) for any of the three to five fully active (supplementary text) LacI-Venus dimers to bind the operator site (Fig. 1B). This implies that the time required

Department of Cell and Molecular Biology, Science for Life Laboratory, Uppsala University, Sweden.

*To whom correspondence should be addressed. E-mail: johan.elf@icm.uu.se

for a single repressor molecule to bind $lacO_{sym}$ is 3 to 5 min. These observations are in excellent agreement with recent theoretical binding-time predictions (3.5 min) based on facilitated diffusion by sliding (*13*) (supplementary text). This overall agreement suggests the possibility of a sliding mechanism, without proving any of the specific assumptions made in the theoretical model.

To directly evaluate whether the *lac* repressor slides on nonspecific DNA sequences in vivo—and if so, how far—we made strains (*15*) with two identical *lac* operator sequences separated by different distances (Fig. 2A, fig. S5, and table S1) and measured how fast the *lac* repressor finds any one of these sites (Fig. 2B). This is an in vivo version of the in vitro assay for TF sliding developed by Ruusala and Crothers (*7*). The rationale is that if the distance between two operator sites is smaller than the sliding distance, they will appear as one search target, whereas two distant operator sites will appear as two independent targets. Indeed, when the two operator sites were positioned 115 base pairs (bp) or 203 bp apart, the first binding event of the two operators occurred twice as fast as the binding event of a single operator (Fig. 2B and fig. S8). This implies that the two operators are perceived as independent targets in the search process and that the sliding distance is shorter than 115 bp. However, when the distance between the operator sites was shortened to 45 or 25 bp, there was a significant decrease in the rate of binding (Fig. 2B), demonstrating that the target regions of the two operators partly overlap. This suggests that the effective target region of an individual operator site is much larger than the ~1 bp precision needed for specific binding by 3D diffusion only (*3*).

To calculate the size of the target region, we derived the association-rate dependence on the operator distance based on the facilitated diffusion model (*3*) (supplementary text and fig. S3). The rate of binding in the two-operator case, r_2, in relation to the rate of binding in the one-operator case, r_1, can be expressed as

$$\frac{r_2}{r_1} = 1 + \tanh\left(L/2s\right) \qquad (1)$$

where L is the center-to-center distance between the operators and $s = \sqrt{D/k_d}$ is the effective capture distance along DNA from each side of one operator. In deriving this relationship, it is assumed that the TF slides along a DNA segment at rate D ($bp^2\ s^{-1}$), that it dissociates from the DNA at rate k_d (s^{-1}), and that the TF always binds as soon as it reaches the operator. The root mean square sliding distance is $s_L = s\sqrt{2}$. A best fit of the association rates in Fig. 2B to Eq. 1 gives an effective sliding distance $s_L = 36 \pm 6$ bp (SEM).

One consequence of sliding on DNA before binding to a specific site is that another protein bound next to the operator would block sliding from that side and therefore reduce the overall association rate by up to a factor of 2. To test this
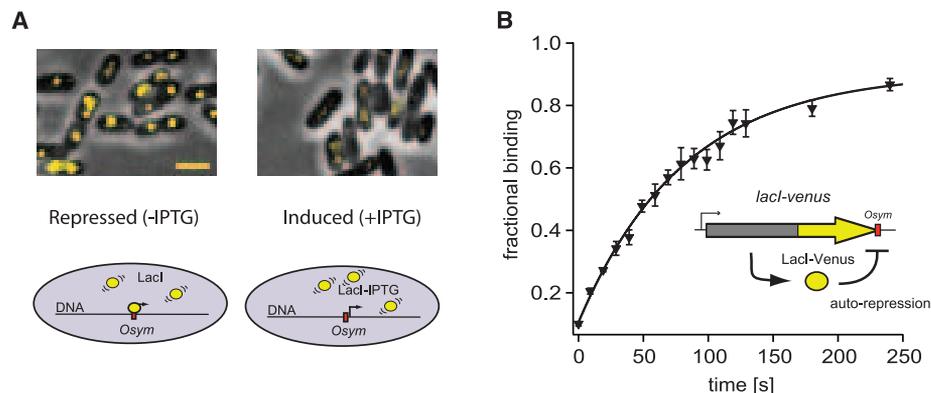

Fig. 1. Single-operator binding assay. (**A**) Overlays of *E. coli* cells imaged in phase contrast and fluorescence microscopy. (Left) Repressing state (−IPTG); LacI-Venus binds the single chromosomal operator ($lacO_{sym}$) and appears as a diffraction-limited spot (yellow). (Right) The cells are induced with IPTG (300 μM), which prevents specific operator binding and results in a diffuse fluorescence signal from the rapidly diffusing LacI-Venus molecules. Scale bar: 2 μm. (**B**) The association rate to a single chromosomal operator is determined by studying the rebinding kinetics of the repressor to the operator after removing the inducer. The fractional binding, i.e., the average number of bright diffraction-limited spots per cell as a function of time, is fitted to the single exponential function $a(1 - be^{-kt})$. (Inset) The accuracy of the assay depends on maintaining a low and even expression of LacI-Venus. This is achieved by using strong autorepression mediated by the ideal *lac* operator $lacO_{sym}$, or $lacO_1$ in a position that overlaps the 3′ end of the *lacI-venus* coding sequence (sequence level information is in table S1).
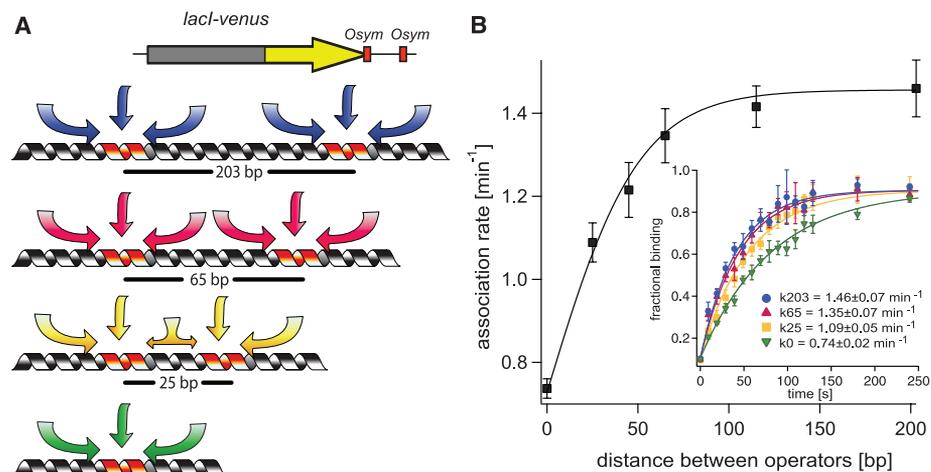

Fig. 2. Sliding-length determination. (**A**) Two identical $lacO_{sym}$ operator sites are positioned at center-to-center distances 25, 45, 65, 115, or 203 bp (45 and 115 bp not shown) in different strains. The capture region of each operator is indicated with colored arrows. When the operators are far apart, they are expected to be independent targets in the search process. When the operators are moved closer, such that the capture regions of two operators overlap, they should appear more and more as one operator site (green). The strains express the same amount of LacI-Venus, as shown by Western blots (fig. S6). (**B**) Rate of binding to the first of two identical operator sites as a function of the interoperator distance. The association rates are fitted to the theoretical sliding length dependence curve (black line), $c(1 + \tanh(L/(s_L\sqrt{2})))$, where L is the distance between operators. $c = 0.73 \pm 0.02$ min^{-1} is the association rate to a single operator, and $s_L = 36 \pm 6$ bp is the sliding distance. Error bars indicate ±SEM; $n \geq 8$. (Inset) Individual association rate measurements (data for 45 and 115 bp are provided in fig. S8).

prediction, we placed the operator $tetO_2$ of the transcription factor TetR next to a single $lacO_{sym}$ operator (Fig. 3A). We optimized the position of the $tetO_2$ site by using molecular-dynamics simulations to place the TetR as close as possible to LacI without allowing contact between the bound proteins (Fig. 3C). When TetR was present, the rate of LacI binding to $lacO_{sym}$ was reduced by

a factor of 1.75 ± 0.18 when the $tetO_2$ site was next to the $lacO_{sym}$ site as compared to when there was no $tetO_2$ site (Fig. 3A). However, the equilibrium binding of LacI to $lacO_{sym}$ was not changed by TetR binding (Fig. 3, A and B, and fig. S14). Thus, TetR obstructs the entry and exit pathways of the *lac* operator without changing the free energy of the bound state.
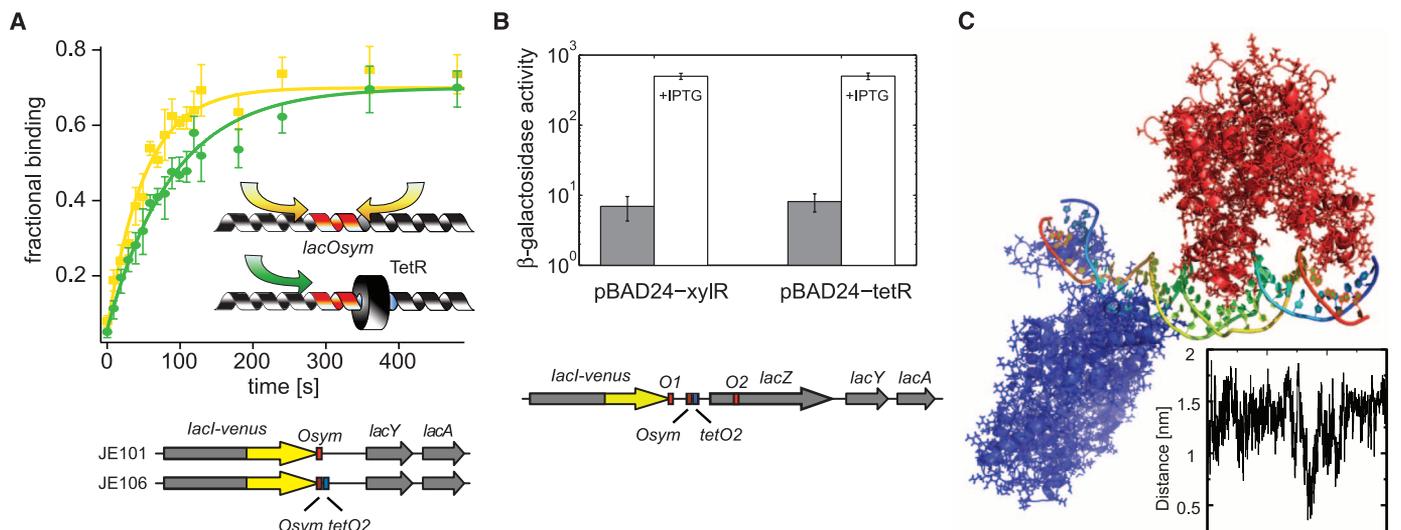
Fig. 3. A TetR roadblock reduces the association rate of LacI without changing its equilibrium binding. (**A**) Single-operator binding kinetics without (yellow squares) and with (green circles) a $tetO_2$ operator site juxtaposed to the $lacO_{sym}$ operator. TetR is expressed from plasmid pQE30 in both strains. The association rates are 1.18 ± 0.09 min^{-1} without $tetO_2$ and 0.68 ± 0.05 min^{-1} with $tetO_2$ (the ratio is 1.75 ± 0.18). Error bars indicate $\pm$SEM; $n \geq 4$. (**B**) β-Galactosidase activity assay showing how the regulation of $lacZ$ is influenced by TetR binding next to the $lacO_{sym}$ as in (A). TetR or XylR is expressed from plasmid pBAD24. (**C**) Molecular-dynamics simulation of LacI (blue) and TetR (red) binding on DNA in the same configuration as in (A) and (B). The simulations are based on crystallographic data of LacI and TetR binding their respective operator. The snapshot image illustrates how the two transcription factors are separated in space. The inset shows how the shortest distance between the proteins changes over time in the simulation.
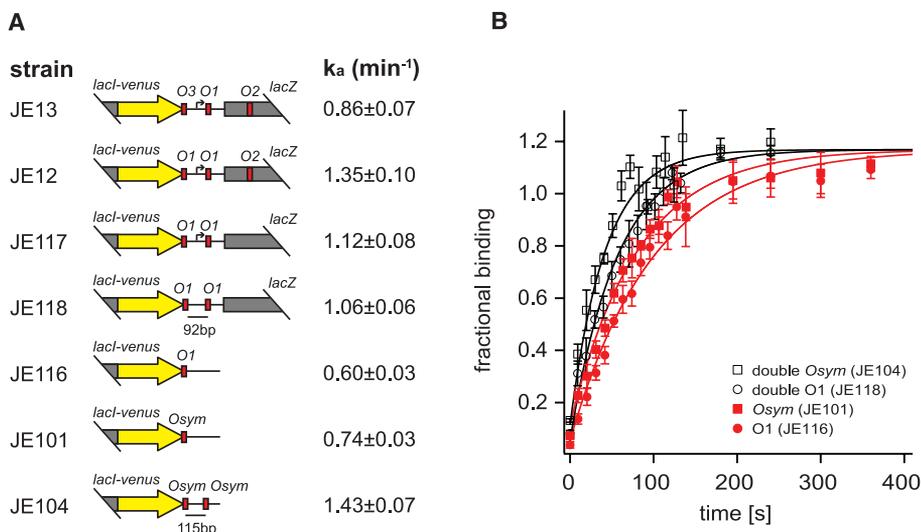

Fig. 4. Contributions from the elements of the wild-type operator region. (**A**) Association rates measured for strains stepwise modified from the wild-type operator configuration in JE13. The arrow indicates the promoter region with binding sites for CRP, H-NS, and RNAP. The contributions of individual operators fit an additive model with $lacO_{sym} = 0.73$ min^{-1}, $lacO_1 = 0.57$ min^{-1}, $lacO_2 = 0.25$ min^{-1}, and $lacO_3 = 0.06$ min^{-1}. See supplementary text for all binding curves and calculations. Error bars indicate $\pm$SEM; $n \geq 4$. (**B**) Comparison of association rates for $lacO_1$ and $lacO_{sym}$ operators. Binding curves are shown for a single $lacO_1$ (red filled circles), a single $lacO_{sym}$ (red filled squares), two $lacO_1$ (black open circles), and two $lacO_{sym}$ (black open squares). Association rates [in (A)] are given by single exponential fits (supplementary text). Error bars indicate $\pm$SEM; $n \geq 4$.

The wild-type *lac* operator region is more complicated than in the simplified constructs. It includes, for example, the binding sites for RNA polymerase (RNAP), cAMP receptor protein (CRP), and histone-like nucleoid structuring protein (H-NS) (*17*, *18*). This raises the possibility that these proteins act like the TetR-roadblock and make sliding less important in the natural context than in our constructs. To identify the contribution of each element in the wild-type *lac* operator region, we modified it stepwise into our artificial construct (Fig. 4A). Starting with the wild-type operator configuration $lacO_3$-O_1-O_2 and changing $lacO_3$ to the much stronger $lacO_1$ operator increased the association rate for the TF to the operator region by a factor of 1.57 (figs. S10, F and H, and S11). Next, the weak $lacO_2$ site was removed from $lacO_1$-O_1-O_2. This decreased the rate of binding only by a factor of 1.20 (fig. S10E), implying that the association rate to $lacO_2$ is lower than to $lacO_1$. Finally, we replaced the binding sites for RNAP, CRP, and H-NS between the two remaining $lacO_1$ sites. This did not change the rate of LacI binding significantly (fig. S10D), showing that the RNAP, CRP, and H-NS sites are not sufficiently occupied to hinder sliding under our experimental conditions.

The rate of binding to the two independent $lacO_1$ operators in the modified *lac* operator region (JE118) is 26% smaller than that to the two independent $lacO_{sym}$ operators (JE104) in the sliding distance experiment (Fig. 4B). This observation is inconsistent with previous theoretical models (*3*, *14*, *19*), which have assumed that the rate of operator binding is diffusion limited and thus independent of variations in operator sequence. The difference was, however, confirmed by comparing association rates to single $lacO_1$ and $lacO_{sym}$ operators in otherwise identical strains (rates: 0.74 ± 0.03 min^{-1} for $lacO_{sym}$ and 0.60 ± 0.03 min^{-1} for $lacO_1$) (Fig. 4B). The difference implies that the repressor has different probabilities, p_{bind}, of binding the different operators before sliding to the neighboring base pair. There are, however, neither theoretical predictions nor experimental estimates of this probability for any TF. Therefore, we have here rederived the established search rate equations to include the probability of

binding the operator (supplementary text and fig. S1). The difference in association rate between $lacO_{sym}$ and $lacO_1$ means that the upper bound for $lacO_1$ is $p_{bind} = 0.12$, if we consider that the upper bound for $lacO_{sym}$ is $p_{bind} = 1$.

One method to determine the absolute value of p_{bind} is to measure association rates to a *lac* operator in strains where roadblocks for sliding have been placed on both sides of the operator (supplementary text). For $p_{bind} = 1$, the overall association rate would be strongly dependent on the distance between the roadblocks because they would determine the effective target region. A $p_{bind} \ll 1$ would imply that the operator is bypassed several times before binding. This would reduce the impact of the roadblocks because the restricted target region would be largely compensated by an increased number of return events (fig. S2). On the basis of measurements with TetR roadblocks at 7 or 12 bp from the *lac* operator, we estimate that $p_{bind}^{O1} = 0.044$ and $p_{bind}^{Osym} = 0.094$ (supplementary text and fig. S13).

It may seem that this low p_{bind} would make the TF search hopelessly inefficient. However, in terms of search efficiency, one has to take into account that the TF returns many times ($s_L/\sqrt{2}$) before leaving the capture region of the operator DNA. In the refined search model, including the low p_{bind}, the sliding distance is $s_L = 45 \pm 10$ bp and the overall probability of binding a $lacO_1$ operator, including multiple return events, is $53 \pm 24\%$ (supplementary text and figs. S1 and S2). One important consequence of $p_{bind} < 1$ is that it invalidates the classical prediction (*3, 19*) that the maximal association rate can be achieved when the repressor spends 50% of the time free in the cytoplasm and 50% nonspecifically bound. When the association rate is maximized for $p_{bind} < 1$, the

optimal fraction of time the TF is nonspecifically bound will be larger than 50% (supplementary text). The experimentally observed 90% nonspecific binding (*14, 20*) is optimal for the lower range of the estimated binding probabilities (supplementary text and fig. S4).

We have demonstrated here that the *lac* repressor slides into its chromosomal operators in living bacterial cells. The average sliding distance is $s_L = 45 \pm 10$ bp, which is close to what is measured in vitro (*5, 7*) for ionic strengths corresponding to 0.15 M monovalent cations (*21*). The sliding makes the search for a $lacO_1$ operator 40 times as fast (Eq. S8) as the situation where the repressor binds DNA nonspecifically but does not slide. In relation to a hypothetical situation where the repressor could bind directly to an operator without nonspecific interactions, the speed-up is a modest factor of 4 (Eq. S14), i.e., the in vivo binding is not much faster than the theoretical diffusion limit for 3D diffusion alone. The fact that the sliding TF does not bind to the operator upon first encounter opens a new level of complexity in the evolution of transcription factors and their binding sites. Indeed, it may be physically impossible to combine a high probability of binding at specific sites with a fast search at nonspecific sites.

References and Notes

1. P. H. von Hippel, O. G. Berg, *J. Biol. Chem.* **264**, 675 (1989).
2. A. D. Riggs, S. Bourgeois, M. Cohn, *J. Mol. Biol.* **53**, 401 (1970).
3. O. G. Berg, R. B. Winter, P. H. von Hippel, *Biochemistry* **20**, 6929 (1981).
4. P. H. Richter, M. Eigen, *Biophys. Chem.* **2**, 255 (1974).
5. D. M. Gowers, G. G. Wilson, S. E. Halford, *Proc. Natl. Acad. Sci. U.S.A.* **102**, 15883 (2005).
6. A. Jeltsch, C. Wenz, F. Stahl, A. Pingoud, *EMBO J.* **15**, 5104 (1996).
7. T. Ruusala, D. M. Crothers, *Proc. Natl. Acad. Sci. U.S.A.* **89**, 4903 (1992).
8. W. T. Hsieh, P. A. Whitson, K. S. Matthews, R. D. Wells, *J. Biol. Chem.* **262**, 14583 (1987).
9. I. Bonnet *et al.*, *Nucleic Acids Res.* **36**, 4118 (2008).
10. P. C. Blainey, A. M. van Oijen, A. Banerjee, G. L. Verdine, X. S. Xie, *Proc. Natl. Acad. Sci. U.S.A.* **103**, 5752 (2006).
11. S. E. Halford, *Biochem. Soc. Trans.* **37**, 343 (2009).
12. R. B. Winter, O. G. Berg, P. H. von Hippel, *Biochemistry* **20**, 6961 (1981).
13. G- W. Li, O. G. Berg, J. Elf, *Nat. Phys.* **5**, 294 (2009).
14. J. Elf, G. W. Li, X. S. Xie, *Science* **316**, 1191 (2007).
15. Materials and methods are available as supplementary materials on *Science* Online.
16. W. Gilbert, B. Müller-Hill, *Proc. Natl. Acad. Sci. U.S.A.* **56**, 1891 (1966).
17. D. Czarniecki, R. J. Noel Jr., W. S. Reznikoff, *J. Bacteriol.* **179**, 423 (1997).
18. S. Rimsky, A. Spassky, *Biochemistry* **29**, 3765 (1990).
19. M. Slutsky, L. A. Mirny, *Biophys. J.* **87**, 4021 (2004).
20. Y. Kao-Huang *et al.*, *Proc. Natl. Acad. Sci. U.S.A.* **74**, 4228 (1977).
21. B. Richey *et al.*, *J. Biol. Chem.* **262**, 7157 (1987).

Downloaded from www.sciencemag.org on August 29, 2015